

Evaluation of downwelling diffuse attenuation coefficient algorithms in the Red Sea

Surya Prakash Tiwari, Y.V.B. Sarma, Burton H. Jones

King Abdullah University of Science and Technology (KAUST), Red Sea Research Center (RSRC),
Biological and Environmental Sciences & Engineering Division (BESE), Thuwal, 23955-6900,
Saudi Arabia

ABSTRACT

Despite the importance of the optical properties such as the downwelling diffuse attenuation coefficient for characterizing the upper water column, until recently no *in situ* optical measurements were published for the Red Sea. Kirby et al.¹ used observations from the Coastal Zone Color Scanner to characterize the spatial and temporal variability of the diffuse attenuation coefficient ($K_d(490)$) in the Red Sea. To better understand optical variability and its utility in the Red Sea, it is imperative to comprehend the diffuse attenuation coefficient and its relationship with *in situ* properties. Two apparent optical properties, spectral remote sensing reflectance (R_{rs}) and the downwelling diffuse attenuation coefficient (K_d), are calculated from vertical profile measurements of downwelling irradiance (E_d) and upwelling radiance (L_u). K_d characterizes light penetration into water column that is important for understanding both the physical and biogeochemical environment, including water quality and the health of ocean environment. Our study tests the performance of the existing $K_d(490)$ algorithms in the Red Sea and compares them against direct *in situ* measurements within various subdivisions of the Red Sea. Most standard algorithms either overestimated or underestimated with the measured *in situ* values of K_d . Consequently, these algorithms provided poor retrieval of $K_d(490)$ for the Red Sea. Random errors were high for all algorithms and the correlation coefficients (r^2) with *in situ* measurements were quite low. Hence, these algorithms may not be suitable for the Red Sea. Overall, statistical analyses of the various algorithms indicated that the existing algorithms are inadequate for the Red Sea. The present study suggests that reparameterizing existing algorithms or developing new regional algorithms is required to improve retrieval of $K_d(490)$ for the Red Sea.

Keywords: diffuse attenuation coefficient, algorithm, evaluation, apparent optical properties, Red Sea

1. INTRODUCTION

The diffuse attenuation coefficient for downwelling irradiance, K_d , is one of the most significant apparent optical properties of seawater that emphasizes how the solar radiation at a particular wavelength is attenuated within the water column^{2,3}. K_d mainly depends on the inherent optical properties (IOPs) and the angular distribution of the surface light field⁴⁻⁶. K_d can be considered as an indicator of the turbidity in the water column⁷, thus, the greater the attenuation of light, the lower the clarity. The clarity of the seawater depends on the concentrations of the in water contents present in a water body.

The biological and physical processes in the water column are dependent on the light field, and the K_d could be described it. The diffuse attenuation coefficient also plays a very critical role to understand the biogeochemical, ecological processes, phytoplankton photosynthesis^{8,9} and photobleaching, and the estimation of primary production in natural waters¹⁰.

$K_d(490)$ is a widely accepted parameter used for various ocean color applications, which has a wide applicability in ocean optics and ocean color remote sensing for instances i) to describe the underwater light field since the depth with enough light for photosynthesis (euphotic depth) can be calculated as $4.6/K_d$; ii) to estimate the “sensed” water column width, as 90% of remotely sensed radiation comes from the layer with a thickness⁷ of K_d^{-1} ; iii) to derive Secchi disk depth from remote sensing data¹¹ which is a water quality parameter used to study the visibility.

Several algorithms for the remote estimation of K_d have been developed for oceanic waters¹²⁻¹⁴. One of the earliest algorithms was developed based on the simple band ratio of water-leaving radiances from the ocean color data of Nimbus-7 Coastal Zone Color Scanner (CZCS) relating $K_d(490)$ ^{12,15}. In previous studies, $K_d(490)$ derived from *in situ*

measurements of K_d at 490 and blue-to-green band ratios of water leaving radiances. Later Mueller and Trees¹³ modified this approach and introduced the ratios of reflectance in blue-green (e.g., 490 and 555nm) that improved the retrieval of K_d at 490nm for the SeaWiFS sensor. Further, Mueller¹⁴ refined his previous algorithm to compute the $K_d(490)$ from the satellite data along with the optimized value of $K_w(490)$ of 0.016 (m^{-1}). This kind of empirical approach has been worked well for various ocean color sensors (SeaWiFS, MODIS, MERIS, OCTS, CZCS) and its operational use with good results over oceanic waters¹⁴. The blue to green ratio is not sensitive in the turbid coastal waters for accurate retrieval of $K_d(490)$. Therefore, recently, Kratzer et al.¹¹ showed the importance of red band (620 nm) to retrieve $K_d(490)$ in the north-western Baltic Sea. Wang et al.¹⁶ improved the method to retrieve satellite-based $K_d(490)$ over oceanic and coastal waters by using the reflectances measured in green and red wavelengths (e.g., 490 and 670 nm). As an alternative to the band ratio algorithms, radiative transfer models have been applied to calculate spectral K_d as a function of IOPs and respective light conditions^{5,17,18}. The radiative transfer based K_d algorithms have been worked well in clear waters and coastal waters¹⁸.

In this paper, we compiled several empirical $K_d(490)$ algorithms and evaluated their performance in the Red Sea using our new dataset. Refer to Table 1 for the description of algorithms used to estimate the diffuse attenuation coefficient in the Red Sea.

Table 1. Description of the algorithms used to estimate the diffuse attenuation coefficient in the Red Sea.

Algorithm Type	General form of Algorithm	Reference
Empirical model with the normalized water-leaving radiance or remote sensing reflectance	$K_d(490) = 0.022 + 0.1 \left(\frac{nL_w(443)}{nL_w(555)} \right)^{-1.29966}$	Mueller and Trees (1997)
	$K_d(490) = 0.016 + 0.15645 \left(\frac{nL_w(490)}{nL_w(555)} \right)^{-1.5401}$	Mueller et al (2000)
	$K_d(490) = 10^{(-0.8515 - 1.8263X + 1.8714X^2 - 2.4414X^3 - 1.0690X^4)} + 0.0166$ with $X = \log_{10}[R_{rs}(490) / R_{rs}(555)]$ (2009 Version)	Mueller et al (2009)
	$K_d(490) = 0.022 + 0.124 \left(\frac{nL_w(443)}{nL_w(555)} \right)^{-1.64}$	Chauhan et al. (2003)
	If $\frac{R_{rs}(490)}{R_{rs}(555)} \geq 0.85$ then $K_d(490) = 10^{(-0.843 - 1.459X - 0.101X^2 - 0.811X^3)}$ with $X = \log_{10}[R_{rs}(490) / R_{rs}(555)]$	Zhang and Fell (2007)
	and $\frac{R_{rs}(490)}{R_{rs}(555)} < 0.85$ then $K_d(490) = 10^{(0.094 - 1.302X + 0.247X^2 - 0.021X^3)}$ with $X = \log_{10}[R_{rs}(490) / R_{rs}(665)]$	
$K_d(490) = -0.05256 + 1.3537 \frac{R_{rs}(670)}{R_{rs}(490)}$	Wang et al. (2009)	

2. DATA

In situ optical measurements

Radiometric properties were measured during in 2014 and 2015 cruises in the Red Sea further referred to as Red Sea Research Center (RSRC) dataset in this paper. The study area and sampling locations are presented in Fig.1. In-water measurements of spectral upwelling radiance (L_u) and spectral downwelling irradiance (E_d) were made by using a SatlanticTM hyperspectral free fall optical profiler named as HyperPro in 350-800 nm wavelength range. Care was taken to avoid overshadowing of the ship during the HyperPro deployments. In air surface radiance (E_s) was measured using a deck reference sensor. The reference sensor was mounted on the top of the ship to avoid any shadowing effects during the cast. Profiles of downwelling irradiance were used to calculate diffuse attenuation coefficient, the first optical depth, photosynthetically available radiation (PAR), and depth of the euphotic zone. A CTD attached with HyperPro measured

temperature, salinity, and the conductivity of the seawater. ECOPUCK embedded with HyperPro, measured the profiles of Chla fluorescence, CDOM fluorescence, and backscattering at the red band (i.e., 700 nm). The remote sensing reflectance ($R_{rs}(\lambda)$) and diffuse attenuation coefficients ($K_d(\lambda)$) were calculated using Prosoft 7.7.16_6 software provided by the instrument manufacturer (<http://www.satlantic.com>). These measurements were made under both clear skies with low solar zenith angle and sometimes Sun covered by clouds. These datasets were acquired at over 49 stations and stored in the system for the further use in algorithm development and validation. In this study, RSRC dataset was used for evaluating the performance of several existing algorithms.

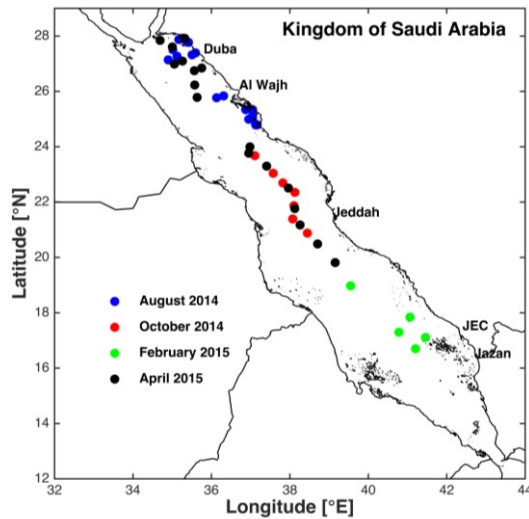


Fig. 1. Location map with station locations in the Red Sea, where the Satlantic HyperPro measurements were collected in during 2014 and 2015.

3. RESULTS AND DISCUSSION

Fig. 2 shows the examples of measured $R_{rs}(\lambda)$ and $K_d(\lambda)$ spectra in the Red Sea. The spectral response of the Red Sea is relatively identical. Most of the $R_{rs}(\lambda)$ have shown a similar trend, with a relatively high reflectance between 0.0015 and 0.009 sr^{-1} at the blue end (400-500 nm), except for few cases showing higher values; an abrupt downward slope starting at around 500 nm due to water absorption, and lower values at the red end of the spectra.

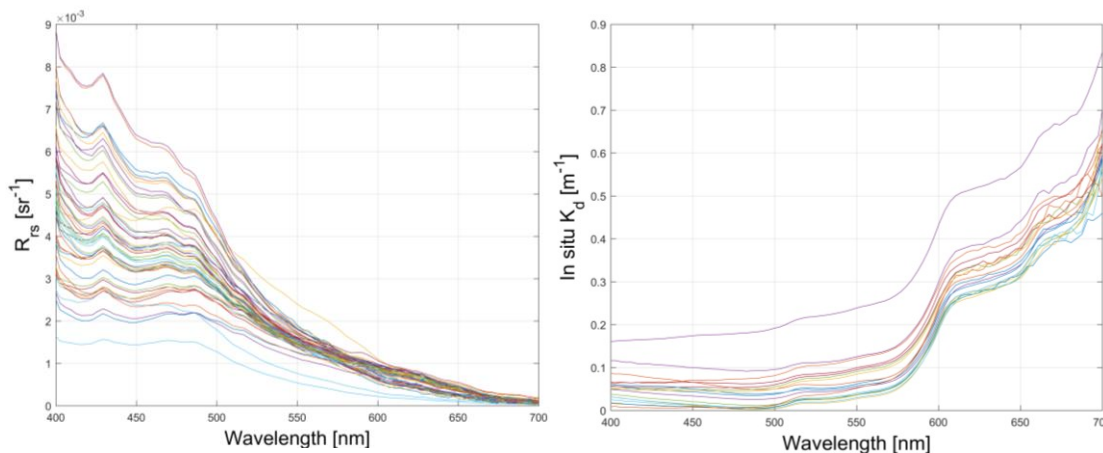


Figure 2. Examples of measured remote sensing reflectance ($R_{rs}(\lambda)$) and diffuse attenuation coefficients ($K_d(\lambda)$) spectra in the Red Sea.

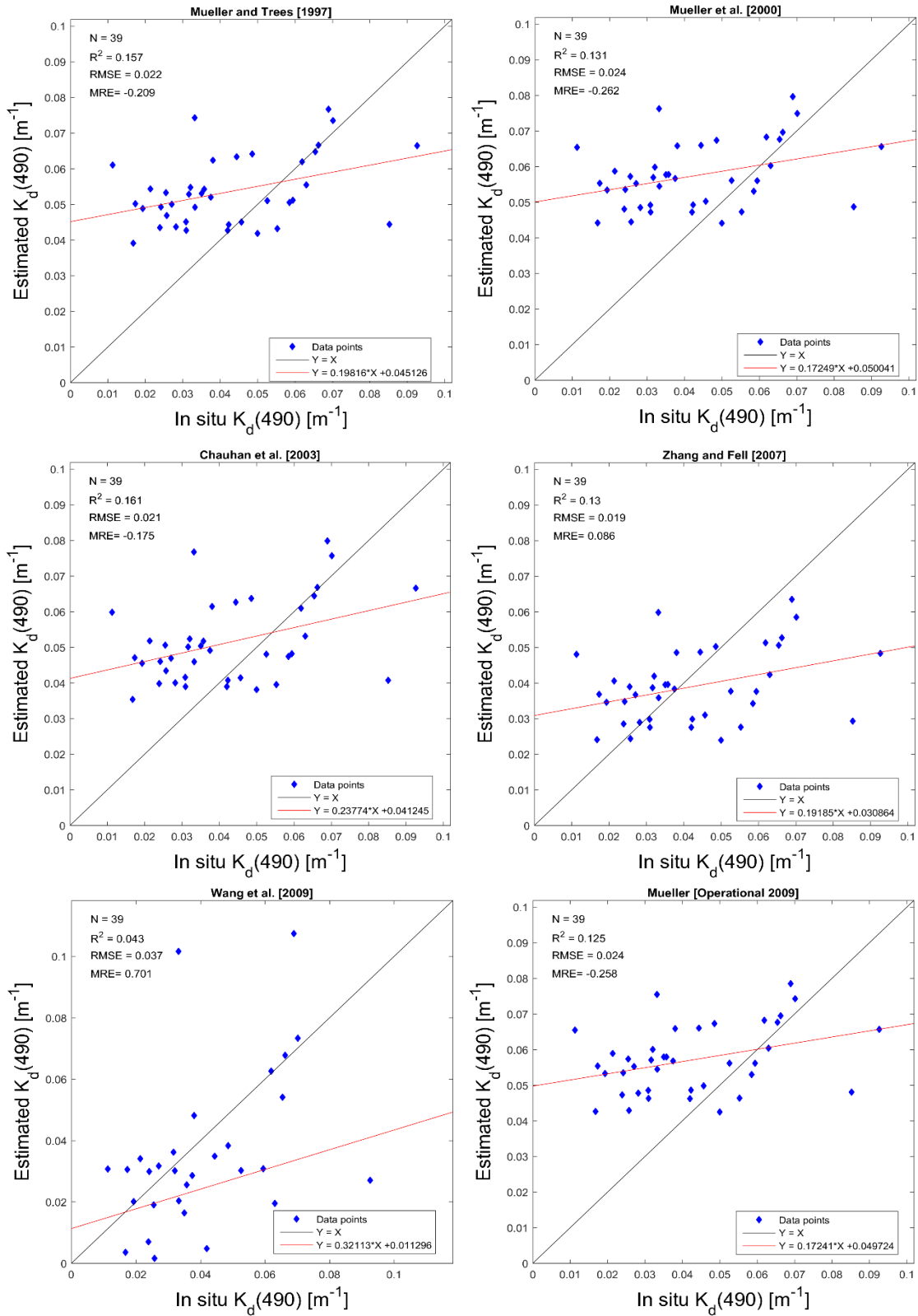


Figure 3. Scatterplots showing comparisons of the estimated $K_d(490)$ [m⁻¹] and in situ $K_d(490)$ [m⁻¹] for RSRC dataset.

The performances of the several algorithms for predicting $K_d(490)$ values were evaluated with RSRC dataset. The statistical evaluation results of these algorithms are shown in the scatter plots. To gain further insight into their performances, scatterplots of the model $K_d(490)$ values versus in-situ $K_d(490)$ values are shown in Fig. 3. A small number of negative values were observed for the Wang et al.¹⁶. These negative values were excluded from the total number of data points (i.e., 49) and finally, 39 valid data points were used to calculate two basic statistical measures (i.e., RMSE and MRE) and correlation coefficient to assess the performance of the algorithms.

Fig. 3 shows the comparisons of the estimated $K_d(490)$ [m^{-1}] and known $K_d(490)$ [m^{-1}] values for the RSRC dataset. When applied to RSRC dataset, these algorithms were overestimated and underestimated against the known values of the $K_d(490)$ with poor linear-linear statistical measures (i.e., RMSE and MRE). Scatter plot for the Zhang and Fell¹⁹ algorithm has the somewhat good statistical measures in terms of the RMSE = 0.019 and MRE = 0.086 with a low correlation coefficient ($R^2=0.13$). Wang et al.¹⁶ algorithm shows the positive mean relative error (MRE = 0.701) with little-improved slope and intercept values with a very low correlation coefficient ($R^2= 0.043$). It also shows little overestimation and underestimation as a comparison of all other algorithms. The highest correlation coefficient ($R^2=0.16$) was achieved by Mueller and Tress¹³ and Chauhan et al.²¹ algorithms. Though the performances of these algorithms on the RSRC dataset were poor and none of the algorithms have shown the good retrieval of $K_d(490)$ [m^{-1}]. It is also noticeable that estimated values of the $K_d(490)$ [m^{-1}] have shown the close matchup with in-situ values at higher $K_d(490)$ [m^{-1}]. Therefore, it appears that these algorithms need to be improved for the low range values of the $K_d(490)$ [m^{-1}] in the Red Sea.

It was noticed that the Wang et al.¹⁶ algorithm appears to have a somewhat better slope and intercept values and tends to produce some negative values in the Red Sea. Earlier studies have suggested that the algorithms for deriving $K_d(490)$ are underestimated/overestimated and produce a negative values in a wide range of waters^{4,11,18-20}. Furthermore, the empirical coefficients can be refined by using regional in-situ optical measurements. This kind of empirical approach has been adopted by various ocean color sensors (OCM, SeaWiFS, MODIS, MERIS, OCTS, CZCS) for operational use with good results over clear open ocean waters. Problems associated with previous studies may be overcome by a neural network algorithm⁶, still its applicability in a wide range of waters needs to be assessed.

4. CONCLUSIONS

In this study, compilations of the several empirical algorithms for deriving the diffuse attenuation coefficient at 490 nm are investigated. These algorithms, collectively as well as individually, are valuable to ocean color community, and they form the basis to understand diffuse attenuation coefficients. These algorithms were applied to RSRC dataset for estimating the diffuse attenuation coefficients and none of the algorithms has shown satisfactory performance in the Red Sea. Some of the algorithm estimated $K_d(490)$ values was comparable against the in situ $K_d(490)$ values, but only at high values of $K_d(490)$. It was noticed that empirical algorithms appear to overestimate $K_d(490)$ in the Red Sea at lower values, whereas Mueller and Trees¹³ and Mueller¹⁴ algorithms tends to produce good results when the diffuse attenuation values were greater than $0.05 m^{-1}$. Our future study will focus on either refining the existing algorithm or developing new parameterizations for the improved retrieval of $K_d(490)$ in the Red Sea.

ACKNOWLEDGMENTS

This study is supported by the King Abdullah University of Science and Technology (KAUST), Kingdom of Saudi Arabia. We thank the operator, master, and crew of *R/V Thuwal*. We would also thanks to M. Ouhssain, B. Kurten, and several other colleagues provided significant help during field work.

REFERENCES

- [1] Kirby, C. M., Parmeter, M. M., Arnone, R. A., and Oriol, R. A., "Optical properties of the Red Sea," No. NOO-TN-03-93, Naval oceanographic office Stennis Space Center MS (1993).
- [2] Preisendorfer, R. W., Hydrologic Optics, vol. 1, Introduction, Natl. Tech. Inf. Serv., Springfield, Va, (1976).

- [3] Tiwari, S. P. and P. Shanmugam, "An optical model for deriving the spectral particulate backscattering coefficients in oceanic waters," *Ocean Science* 9, no. 6, 987-1001 (2013).
- [4] Morel, A., Huot, Y., Gentili, B., Werdell, P. J., Hooker, S. B., and Franz, B. A., "Examining the consistency of products derived from various ocean color sensors in open ocean (Case 1) waters in the perspective of a multi-sensor approach," *Remote Sensing of Environment* 111, 69–88 (2007).
- [5] Kirk, J. T. O., "Dependence of relationship between inherent and apparent optical properties of water on solar altitude," *Limnology and Oceanography* 29, no. 2 350-356 (1984).
- [6] Jamet, C., Hubert, L., and Dessailly, D., "Retrieval of the spectral diffuse attenuation coefficient $K_d(\lambda)$ in open and coastal ocean waters using a neural network inversion," *Journal of Geophysical Research: Oceans* 117, no. C10 (2012).
- [7] Kirk, J. T. , *Light and photosynthesis in aquatic ecosystems*. Cambridge university press, (1994).
- [8] Platt, T., "Primary production of the ocean water column as a function of surface light intensity: algorithms for remote sensing." *Deep Sea Research Part A. Oceanographic Research Papers* 33, no. 2, 149-163 (1986).
- [9] Sathyendranath, S., Platt, T., Caverhill, C. M., Warnock, R. E., and Lewis, M. R., "Remote sensing of oceanic primary production: Computations using a spectral model," *Deep Sea Research Part A* 36, 431–453 (1989).
- [10] Yu, X., Salama, M. S., Shen, F. and Verhoef, W., "Retrieval of the diffuse attenuation coefficient from GOCI images using the 2SeaColor model: A case study in the Yangtze Estuary." *Remote Sensing of Environment* 175, 109-119 (2016).
- [11] Kratzer, S., Brockmann, C., and Moore, G., "Using MERIS full resolution data to monitor coastal waters: A case study from Himmerfjärden, a fjord-like bay in the northwestern Baltic Sea," *Remote Sensing of Environment* 112, 2284–2300 (2008).
- [12] Austin, R. W. and Petzold, T. J., "The determination of the diffuse attenuation coefficient of sea water using the Coastal Zone Color Scanner," In *Oceanography from space*, Springer US, 239-256. (1981).
- [13] Mueller, J. L. and Trees, C., "Revised SeaWiFS prelaunch algorithm for diffuse attenuation coefficient $K(490)$," *Case Studies for SeaWiFS Calibration and Validation* 41, 18–21 (1997).
- [14] Mueller, J. L., "SeaWiFS algorithm for the diffuse attenuation coefficient, $K(490)$, using water-leaving radiances at 490 and 555 nm," *SeaWiFS postlaunch calibration and validation analyses, Part 3*, no. 11, 24–27 (2000).
- [15] Austin, R. W. and Petzold, T. J., "Spectral dependence of the diffuse attenuation coefficient of light in ocean waters." *Optical Engineering* 25, no. 3, 253471-253471(1986).
- [16] Wang, M. H., Son, S. and Harding, L. W., "Retrieval of diffuse attenuation coefficient in the Chesapeake Bay and turbid ocean regions for satellite ocean color applications," *Journal of Geophysical Research* 114, no. C10 (2009).
- [17] Gordon, H. R., "Dependence of the diffuse reflectance of natural waters on the sun angle," *Limnology and Oceanography* 34, 1484-1489 (1989).
- [18] Lee, Z. P., M. Darecki, M. K. Carder, K. L., Davis, C. Stramski, D., and Rhea, W., "Diffuse attenuation coefficient of downwelling irradiance: An evaluation of remote sensing methods," *Journal of Geophysical Research* 110, no. C2 (2005).
- [19] Zhang, T. L. and Fell, F., "An empirical algorithm for determining the diffuse attenuation coefficient K_d in clear and turbid waters from spectral remote sensing reflectance," *Limnology and Oceanography: Methods* 5, 457–462 (2007).
- [20] Tiwari, S. P. and Shanmugam, P., "A robust algorithm to determine diffuse attenuation coefficient of downwelling irradiance from satellite data in coastal oceanic waters," *Selected Topics in Applied Earth Observations and Remote Sensing, IEEE Journal of* 7, no. 5, 1616-1622 (2014).
- [21] Chauhan, P., A. Sahay, A., A. S. Rajawat, A. S., and Nayak, S., "Remote sensing of diffuse attenuation coefficient (K_{490}) using IRS-P4 Ocean Color Monitor (OCM) sensor," *Indian Journal of Marine Sciences* 32, 279–284 (2003).